Evaluating a calibration method for the estimation of fragmented rocks 3D-size-distribution out of 2D images

S. Outal
University of Liège (ULg), GeMMe-MiCa, Liège, Belgium

J. Schleifer
MINES Paristech, CMM, Centre de Géosciences, Fontainebleau, France

E. Pirard
University of Liège (ULg), GeMMe-MiCa, Liège, Belgium

ABSTRACT: Image analysis is a tool having great potential for the quantification of fragmented rocks size-distribution. This recent technique should be validated according to sieving measurements. Current acquisition allows the obtaining of only 2D information from images. In addition, the 3D passage is extremely problematic. Firstly, the usual stereological methods do not work because the reasoning is carried out on non-random projections. Secondly, estimated sizes differ from those measured by sieving. Last, a quantity of material measured during sieving remains inaccessible by image analysis, due to masking and segregation. This paper evaluates a method directly connecting 2D raw data to 3D sieving measurements. The cited problems are reduced as much as possible thanks to the adoption of an isotropic 2D sorting criterion, and thanks to samples without masking and segregation. Important results have been obtained. Firstly, the characteristic size is correctly estimated in 2D, giving access to computing the uniformity index through known models. Secondly, the stereological approach, bringing into play proportions, is not sufficiently robust to reconstruct easily volume distributions. Limits of this kind of methods, which are, unfortunately, currently used in several granulometric applications, are analyzed.

1 INTRODUCTION

These last years the measurement by image analysis of quantitative parameters has been developed with the evolution of data processing and with new developments carried out in image processing. Nevertheless, image analysis being a new and a concurrent measurement technique is often faced with evaluations via its comparison with reference measurement systems.

In the case of the quantification fragmented rocks size-distribution, the reference system is sieving. It provides a measurement of fragment sizes and their equivalent masses (or volumes for materials with a constant density). Consequently, to perform the validation of image analysis results, 2D data measured on fragmented rocks images must be correctly converted in sizes and volumes. However, except the extraction of the 2D information itself (projected areas of fragments), the volume reconstruction is precisely one of the main issues encountered in the estimation of the fragmented rocks size-distribution by image analysis. The problem leads to the fact that sizes and the volumes estimated by image analysis (without calibration) differ largely from those of sieving.

Firstly, images, acquired in video mode, represent projections of fragments visible areas coded in 256 grey levels. The shape of fragments is rather complex. Thus their projected areas, whose form depends on the angle of acquisition and the way they rest on the surface of the heap, are not representative neither for their sizes nor for their volumes. Also, since the reasoning occurs in projections (not on cross sections) obtained in a non-random way; the usual stereological methods do not work.

Secondly, size concepts of the two measurement systems are not similar. Indeed, the attribution of the size when it acts of the sieving is carried out with answering the simple question: will the fragment pass through a given mesh or not? This passage depends obviously on all spatial dimensions of the fragment (globally: width, and thickness). On the other hand, it is completely different for image analysis. Indeed, the extraction of fragment contours gives access to its 2D projected area. Even if one considers that the fragment rests gravitationally on its largest side, it is too difficult to define the square sieve mesh by which it will be retained. Various sizes can be considered according to the third dimension of the fragment, which is unfortunately inaccessible by the current acquisition (Fig. 1). Though, good correlations are obtained for powders but only when used sieves are of rounded meshes (Pirard et al. 2004).

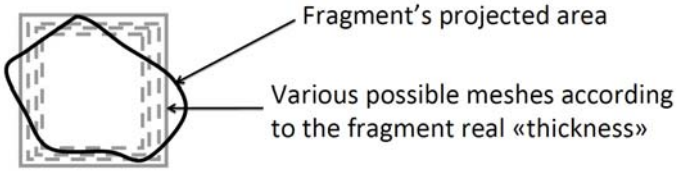

Figure 1. Various possible meshes by which the same projected area can theoretically pass.

Thirdly, the volume reconstruction is accompanied by the interference of various problems:

- Because of the different conditions met during the formation of the analyzed heap, the images represent fragments masked between them, or not presenting their largest projected areas to the camera. In deed, if one is interested in the establishment of correct correlations between fragments volumes and their projected areas, one must necessarily consider their largest projected area.
- The segregation undergone by fragments having small sizes is the second problem. While these fragments are accessible during the sieving operation and are consequently weighed, they still inaccessible during image analysis because they do not appear on the surface of the image. An undervaluation of their proportions is thus inevitable while establishing the size-distribution by image analysis (systematic bias).
- The third problem is related to the covering thickness equivalent to the various layers of fragments which form the analyzed heap. The first layer measured by image analysis does not certainly inform about the entirety of the heap.
- The last problem is related to the 2D treatments phase when errors of fusion of small particles and over-segmentation of large fragments appear. They are reflected by skewed calculations of fragment sizes and volumes (analytic bias).

The most known methods for sizes calculation by image analysis use a 3D modelling of the fragment shape. They assume that its projected area correctly represents the projection of its total form in the plan of the image. It is the case for the spheres model used in the software FragScan (Chavez 1996, Schleifer & Tessier 1996). The algorithm uses partial contours of the fragments. The reasoning is thus rather based on the notion of size classes. A projected area, which is equivalent to a given class and obtained through the application of two successive morphological openings, is supposed to represent the projection of a number of spheres of a given diameter.

There are also other methods, which are based on the adjustment of the complex shape of the projected area to a simple geometrical form. Kemeny et al. (1999) while referring to calibration tests with the sieving, assign to each projected area a size known as Screen size (S_s) computed in the following way:

$$S_S = \sqrt{A_{ma} \times A_{mi}} \quad (1)$$

In this equation, A_{ma} and A_{mi} are the two axes of the "Best fitting ellipse" of the fragment projected area. The volume of the fragment is then considered as being its S_s multiplied by its projected area. Let us note nevertheless that, if one considers the disc of diameter d and the ellipse of the same area (thus of the fragment projected area), it appears that it is not necessary to proceed by the determination of a "Best fitting ellipse". Indeed, S_s and the volume (V_f) of the fragment can be given simply by:

$$S_S = d \qquad \text{and} \qquad V_f = \left(\frac{\sqrt{\pi}}{4}\right).d^3 \quad (2)$$

Maerz (1996) in his work on the quantification of the fragmented rocks distribution by image analysis uses equations that result from the stereological theory of the integral geometry (Santalo 1976). He is inspired by the fact that the calculation of intercept by plans on fragments allows to establish the distribution of their projected areas. The author tries thereafter to connect this distribution to the reference with the help of an unfolding function. Nevertheless, due to the difficulty to correctly operate this reconstruction, the author emits some simplifying assumptions, but certainly strong enough for some of them. In addition, the information of projected areas does not correspond to that obtained following a cut by a given plan. This also leads the author to operate series of comparisons with sieving, which allow him to calculate coefficients of calibration. However, the author is not explicit concerning, neither the adopted size concept, nor the method followed for the computation of volumes.

In addition, no matter which approaches for size calculation and volumes reconstruction are used, shifts between the distribution estimated by image analysis and its reference are attributed partly to the segregation of small sized fragments (Ouchterlony et al. 1990), and to the sampling procedure (Hunter et al. 1990). In the same way, to eliminate these shifts, calibration coefficients are introduced based on comparisons with the sieving. They are characterized to be non-robust for the majority of cases. Indeed, Conditions under which they are established seem to change, not only from one heap to another, or from one sample to another, but also from one image to another.

The volume reconstruction method studied in this paper is defined as an anamorphosis. It is a question of working out a transfer function, which will connect directly the rough 2D proportions of projected areas (without reconstruction of forms), calculated by image analysis, to the volume proportions measured by sieving. In theory, this transfer function, es-

tablished on a calibration sample acquired under controlled conditions (lighting, dispersion of fragments, no segregation, etc.), should enable us to reconstruct the volume size-distributions of other samples acquired under the same conditions.

2 METHOD

2.1 *Computing the transfer function*

We consider an experimental sample of fragmented rocks that have a constant density. On one hand, the sieving allows us to sort the fragments according to square sieve meshes and to compute the 3D-size-distribution (P_{3D}), which represents the 3D-sizes, r_{3D}, weighted by the volumes. On the other hand, image analysis performed on the same sample allows us to delineate contours of fragments (Fig. 3b, d), and then to compute its 2D-size-distribution (P_{2D}), which represents the 2D-sizes, r_{2D}, weighted by the projected areas.

The purpose is to find a transfer function Q that connects the two distributions P_{2D} and P_{3D}. The computation of Q will allow us in theory to compute P_{3D} in the case when we do not have access materially to fragments to sieve them (only P_{2D} is available). This may be the case when taking the measurement under industrial environment (mines, quarries, etc.). Images can then be acquired over the belt conveyer, over loading machines or even on the blasted muckpile. If such function exists, then for each given size r, it will verify the following equation:

$$P_{3D}(r) = P_{2D}(Q(r)) \tag{3}$$

In this paper, we consider the determination of Q in the case when the experimental samples are prepared in such way that P_{3D} obeys the Rosin-Rammler model (Peleg 1996). This model is frequently selected when it acts of estimating the fragmentation using image analysis. Coupled, with some precautions, to Kuznetsov equation, this model has been used for calculating the fragment size distribution in a blasted muckpile (Cunningham 2005). It expresses the volume cumulative passing by:

$$P(x) = 1 - \exp\left(-\left(\frac{x}{X_c}\right)^n\right) \tag{4}$$

Where X_c is the characteristic size of the distribution. And, n is the uniformity index; it provides an indication of the stiffness of the size-distribution curve.

As it will be observed experimentally (section 4.1), when P_{3D} is fit properly to Rosin-Rammler, then P_{2D} also is properly adjusted to this model. Accordingly, the transfer function Q is necessarily a power function. So, when two given cumulative passing P_{2D} and P_{3D} are equal, then the two equivalent sizes r_{2D} and r_{3D} are connected by the following relationship:

$$r_{2D} = X_{c2D}\left(\frac{r_{3D}}{X_{c3D}}\right)^{\left(\frac{n_{3D}}{n_{2D}}\right)} \tag{5}$$

It follows that the function Q is written in the form:

$$Q(r) = X_{c2D}\left(\frac{r_{3D}}{X_{c3D}}\right)^{\left(\frac{n_{3D}}{n_{2D}}\right)} = k.r^{\alpha} \tag{6}$$

In practice, when we have a calibration sample, image analysis and sieving will make it possible to determine the two parameters k and α. Then, for other cases where only P_{2D} is accessible the estimation of P_{3D} through anamorphosis can be calculated by:

$$P^*_{3D}(r) = P_{2D}(k.r^{\alpha}) \tag{7}$$

Estimating P_{3D}^*, using 2D-data extracted by image analysis, allows us to compute the two parameters k and α. This is done with adjusting the equivalent experimental points of P_{3D}^*, plotted in a log-log network, to a straight line.

In other respects, the evaluation of the robustness of the transfer function is performed on an experimental sample by comparing P_{3D}^* (estimated by image analysis) to P_{3D} (measured by sieving).

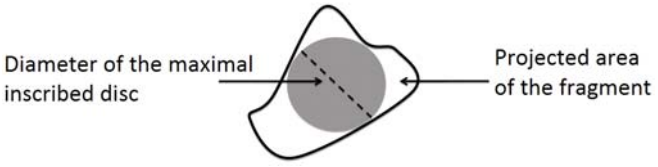

Figure 2. Sorting criterion of projected areas adopted by image analysis.

2.2 *Sorting criterion adopted by image analysis*

In the case of image analysis we must define a sorting criterion to assign a 2D-size (r_{2D}) to each projected area. First of all, the determination of the fragments contours consists of morphological filtering followed by a relevant delineation of fragments contours (Outal 2006, Beucher 2007). The resulting image is then a binary image that represents projected areas of various size fragments, separated by a black space corresponding to empty zones (Fig. 3b, d). The size that we assign to each projected area is the diameter of the maximal inscribed disc in its interior (Fig. 2). We have to notice that this is not a question of a size concept itself but rather an isotropic method of sorting. In this stage of resolution, 2D-sizes of projected areas are not final sizes but rather sizes, which allow classifying them in 2D.

Sieving sizes (r_{3D}), will be calculated thereafter when using the transfer function Q.

3 MATERIAL

Two experimental batches will be used. The first is intended to estimate by image analysis the two parameters X_c and n, and for the detailed evaluation of the transfer function method used for the estimation of P_{3D}^*. The second batch, made up of a another type of rock, will be used to validate the recovery of X_c.

The first batch relates to nine granulometric size-distributions named P01, P09… P67. They come from the Department of Engineering of Queen Mary & Westfield College (Latham et al. 2003). Each of the nine distributions represents a population of fragments of the same type of rock, and weighs about 30 kg. Before the acquisition, the majority of fragments whose sizes are included in the interval [1 mm; 125 mm], show their largest area to the camera, and are laid out with a minimum of masking (Fig. 3a). Each distribution is represented by an individual image. The volume refusals were prepared so that the size-distribution of each distribution (image) follows exactly the Rosin-Rammler model with a given set of parameters X_{c3D} and n_{3D}. The 3D here corresponds to volumes measured by sieving (Table 1). Projected areas are obtained using automatic delineation algorithms to the nine images (Fig. 3b).

The second batch was built by our care in the centre of Geosciences at the École des Mines de Paris in 2005. It relates to black schist resulting from crushing and coming from the mine of Merlebach located in the Lorraine coalfields (France). A mass of 9050 g was sieved using twelve screens of 2 and 25 mm. In the same way, the volume refusals of the batch were conceived so that the total distribution follows the Rosin-Rammler model (Table 1). After sieving, the fragments were mixed and subsequently dispersed along one layer without overlap amongst them. They are also laid out in order to have their largest side below the camera. The acquisition gave place to nine images (P1, P2... P9) forming a mosaic of the entire distribution. Each image represents a part of the whole of this second batch (Fig. 3c).

3.1 *Scenarios analysed*

Since the batch N°1 is composed of nine distributions of different sizes, we separated evaluation tests of the transfer function in three scenarios that simulate industrial conditions of calibration (a small calibration sample that represent a great muckpile).

– The first case of figure is that of the nine granulometric distributions considered separately, and for which the distribution P10 is taken as the calibration sample. The other eight distributions will successively play the role of the blasted muckpile.
– The second corresponds to the formation of a single heap resulting from the regrouping of the eight size-distributions equivalent to images P01, P09, P14, P29, P32, P46, P49 and P67. The adjustment of the cumulative passing of the joined eight distributions to Rosin-Rammler model gave the following set of parameters: X_{c3D} (single Heap) = 41.29 mm and n_{3D} (single Heap) = 0.92. P10 is also considered the calibration sample and the single heap will be considered the blasted muckpile.
– Lastly, the third case of figure consists in gathering the nine sizes distributions into two distinct heaps: The Heap N°1, which will be considered the calibration sample, is composed of the four distributions P32, P46, P49 and P67. The adjustment of the experimental volume passing measured by sieving the Heap N°1, gave the following parameters: X_{c3D} (Heap1) = 34.34 mm and n_{3D} (Heap1) = 0.73. The Heap N°2 consists of the five remaining distributions P01, P09, P10, P14 and P29, with X_{c3D} (Heap2) = 50.72 mm and n_{3D} (Heap2) = 1.31.

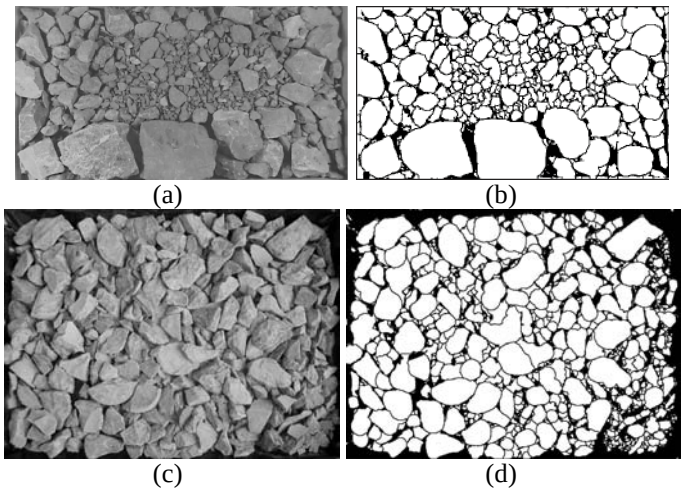

Figure 3. (a) Grey level image of P29 from batch N°1 and (b) binary image representing the projected areas. (c) Grey level image of P1 from batch N°2, and (d) binary image representing the projected areas.

4 RESULTS AND DISCUSSION

The steps of the recovery of X_{c2D} by image analysis are the following. The application of successive morphological openings by reconstruction, of increasing sizes, on projected areas, makes it possible to sort them according to 2D-sizes classes. The size of each projected area (maximum disks inscribed) is equivalent to the size of the opening which eliminates it. And its surface is the sum of pixels that constitute it. P_{2D} is then computed. After that, the adjustment of the experimental data of P_{2D} to Rosin-

Rammler is used to calculate X_{c2D} and n_{2D} of each batch (Tables 1 and 2).

Table 1. 2D and 3D Parameters of the Rosin-Rammler model successively computed by image analysis and measured by sieving (Batch N°1: 1st case).

	Batch N°1 (1st case)								
	P01	P09	P10	P14	P29	P32	P46	P49	P67
X_{c3D} (mm)	64.9	42.4	62.3	25.4	66.8	20.6	30.5	59.8	36.9
n_{3D}	1.76	1.59	1.34	1.77	0.91	1.32	0.89	0.70	0.49
X_{c2D} (mm)	65	40.8	52.7	28.2	62.1	27.8	37.2	56.9	47.8
n_{2D}	2.01	2.11	1.69	2.27	1.19	2.15	1.75	1.17	0.92

Table 2. 2D and 3D Parameters of the Rosin-Rammler model successively computed by image analysis and measured by sieving (Batch N°1: 2nd, 3rd cases, and Batch N°2).

	Batch N°1			Batch N°2
	2nd case	3rd case		
	Single Heap	Heap N°1	Heap N°2	
X_{c3D} (mm)	41.3	34.3	50.7	14.7
n_{3D}	0.92	0.73	1.31	2.5
X_{c2D} (mm)	44.2	37.7	47.9	12.8
n_{2D}	1.25	1.19	1.48	1.88

4.1 *Characteristic size X_c*

The Adjustments to the Rosin-Rammler model carried out on 2D data show that the granulometric distributions of projected areas also follow this model. This result can be explained by the fact that 2D measurement is performed on images not presenting masking. Another element is that each visible fragment on the image is laid out gravitationally in such a way that it presents its largest projected area during measurement. Thus, the good representativeness of images obtained through a controlled provision of fragments seems to allow the conservation of the correct adjustment to the Rosin-Rammler model.

In addition, the comparison of X_{c2D} and X_{c3D}, related to the three scenarios of the batch N°1, shows that the order of magnitude of X_c is properly extracted in 2D. This is verified for almost all studied granulometric distributions. The same observation can be made for the batch N°2, which is formed by another type of rock, and is obtained under different conditions of fragmentation. This last fact constitutes a validation of this other experimental result.

Image analysis thus allowed the correct extraction, without passage in 3D, of the characteristic size X_c, and this exceptionally when analyzed images are representative. It appears that the information contained in the projected areas is sufficient for the quantification of this parameter in 2D, for the type of fragment shapes studied and their equivalent representative images. X_c can also be suitably approximated under industrial conditions of measurement. Specially, this can be done for fragmented rock images acquired on conveyors belts. Indeed, the vibration caused by the movement makes it possible to separate fragments amongst them as much as possible and allows gravitationally dispersing them on their largest area. In addition, the choice of a transport speed of materials higher than that of their fall on the belt will make it possible to have a single layer moving during analysis.

4.2 *Uniformity index n*

On the other hand, for almost all granulometric distributions, the uniformity index n_{2D} calculated by image analysis is higher than that of reference, measured by sieving. The result is that the estimated size-distribution-curves are “steeper” than the reference. The uniformity, n, of distributions cannot then be estimated suitably by image analysis, as the case for the characteristic size, X_c. It appears that the recovery of this parameter depends on the third dimension information, which is inaccessible due to the current acquisition. In practice, for measurements in industrial conditions, it would be useful to proceed as follows: initially, the processing of 2D data remains very useful for the correct extraction of X_c as shown above. Then, uniformity n could be quantified using geometrical parameters related to the blasting pattern adopted during the rock fragmentation process. To do this, the well-known Kuz-Ram model could be used (Cunningham 2005).

4.3 *Evaluation of anamorphosis*

The objective now is to try to reconstruct the volume distribution using the anamorphosis applied to projected areas. Data handled are those relative to the three cases of figures of the batch N°1. For the two first cases of figures, parameters k and α of anamorphosis related to the P10 distribution are calculated using the Equation 6 (Table 3). Then, estimations of volume cumulative passing P_{3D}^* of the eight hypothetical blasted muckpiles are calculated based on Equation 7. The same procedure, applied to the third case of figure, allows to compute P_{3D}^* for the Heap N°2. All P_{3D}^* are then compared with references (P_{3D}) in a log-log network (Figs 4, 5).

For practically all studied cases, volume distributions resulting from anamorphosis follow the same trends as those of reference, but differ in proportions. Indeed, only the volume proportions of distributions P09, P14 and P29 appear to approach suitably the reference. Nevertheless, the examination of parameters related to projected areas and volumes of these three distributions does not make it possible to detect any particularity, compared with other distributions parameters. Thus, for the first two cases of

figures, parameters k and α of P10 are not stable enough to be able to reconstruct the other distributions. Indeed, volume proportions of all other distributions are underestimated by anamorphosis, giving place to granulometric distributions characterized by elements coarser than those of reference. In the same way, for the third case of figure, parameters k and α of the Heap N°1 are not stable too. For this case, volume proportions are over-estimated what gives place to finer curves compared with reference.

Table 3. Anamorphoses parameters of the experimental batch N°1: three cases of figures.

	1st case of figure (Nine distinct distributions) & 2nd case of figure (Single Heap)	3rd case of figure (Heap n°1 & Heap n°2)
	P10	Heap N°1
k	1.99	4.31
α	0.70	0.61

So in all cases, the anamorphosis is not robust and is insufficient to correctly describe characteristics that connect 2D data extracted by image analysis to 3D data measured by sieving. This finding is confirmed by the fact that results was noted on various cases of figures representing the same type of rock for which problems of masking and sampling have been experimentally avoided. In the same way, problems likely to be related to a poor extraction of the 2D information of projected areas have been avoided with the help of relevant fragments delineation (Fig. 3b, d). Thus, described insufficiencies are not a problem related to image-processing. This inability of anamorphosis to operate a correct 3D reconstruction can be explained by the fact that being established on proportions adjusted to a mathematical model, the anamorphosis appears eliminating all material concepts (projected areas and volumes), which characterize studied granularities. It is rather associated with a transfer function than a reconstruction law. Variations noticed between comparison curves show that anamorphosis informs rather about the relation between the whole of 2D proportions on one side, and 3D proportions on another. The result of the application of the method thus depends on the distribution of fragmentation within studied classes. In this way, a loss of robustness and stability of anamorphosis parameters is noted when granulometric proportions vary from one distribution to another. Nevertheless, various aspects and skews seem to be treated by this transfer function. Indeed, in addition to the volume information of reconstruction contained in anamorphosis computations, skews due to the difference in size concepts between the two systems of sorting are also taken into account over all size-classes. Consequently, variation of concerned sizes from one distribution to another seems to affect the robustness of the method.

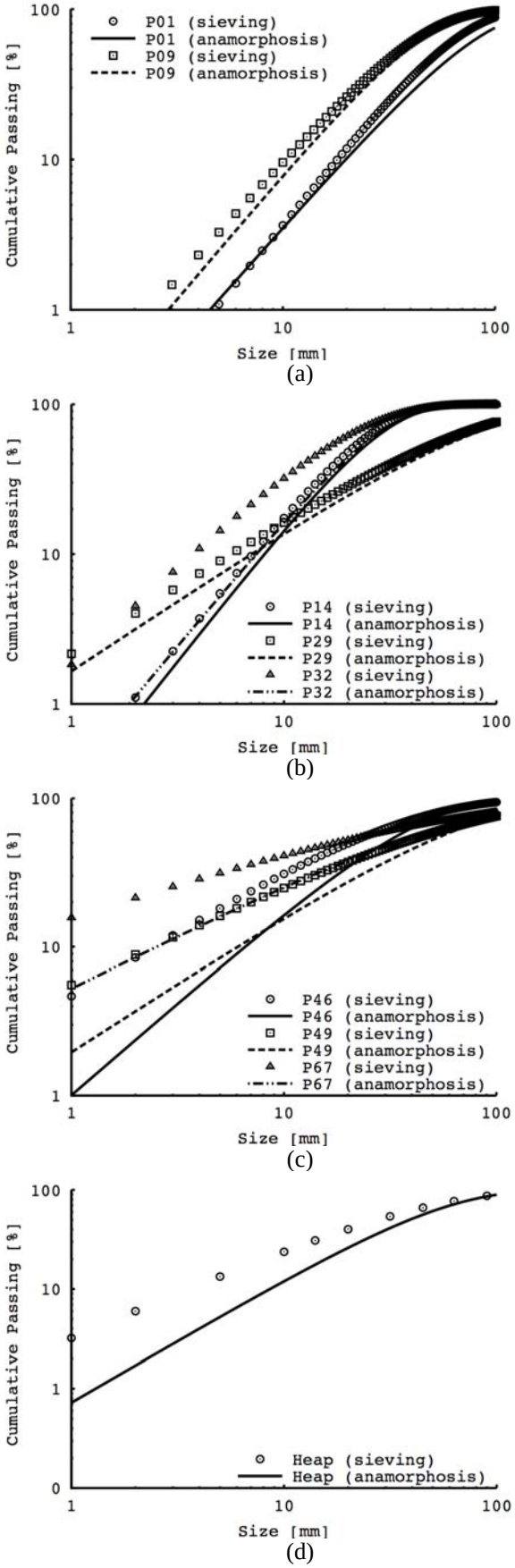

Figure 4. Results of the application of anamorphoses to projected areas when P10 is the calibration sample. (a), (b), (c) Nine distributions, (d) Single heap.

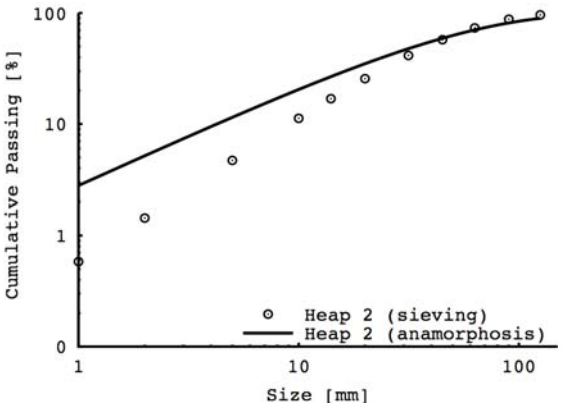

Figure 5. Results of the application of anamorphoses to projected areas when heap N°1 is the calibration sample. Heap N°1 and Heap N°2.

5 CONCLUSION

Two experimental batches of fragmented rock distributions, adjusted to the Rosin-Rammler model, were analyzed jointly by two systems of measurement: image analysis and sieving. The latter is the reference of the measurement of fragmented materials size-distribution.

In grey level image analysis, since we do not have access to the third dimension of fragments, the sorting of projected areas was made in the most possible isotropic way, and this through choosing the maximum inscribed discs inside projected areas.

Initially, the study of representative images has allowed a correct extraction of the characteristic size X_c. This was made possible because two essential conditions were observed:

– The first concerns the avoidance of masking and sampling problems with the help of the analysis of only one layer and the measurement of the totality of the sample together with image analysis and sieving. Moreover, fragments present their larger projected area to the camera.
– The second relates to the avoidance of image processing problems inherent to erroneous 2D-information (fusion and over-segmentation). This was possible thanks to relevant delineation of visible fragments on images.

Then, under these same conditions, the anamorphosis method has been evaluated in detail concerning the 3D reconstruction starting from 2D data. On one hand, tests carried out showed that the method is not robust, because the information managed by the transfer function seems to take into account various non-stable skews from one distribution to another. Thus, for the majority of cases, obtained curves follow the same trends as those of reference, but with underestimated volume proportions. On the other hand, the fact that the method operates on proportions eliminated all the material concepts. Indeed, an analysis based on a material concept is essential for a good interpretation as well as for 2D projected areas, as for 3D volume data. Our work bringing into play material concepts through the reasoning on the refusals histogram, instead of cumulative passing, seems to confirm the relevance of this idea (Outal 2006, Outal et al. 2008).

REFERENCES

Beucher, S. 2007. Numerical residues. *Image and Vision Computing* 25(4): 405-415.

Chavez, R. 1996. Mise au point d'outils pour le contrôle du tir à l'explosif sous contraintes de production. PhD thesis, École des Mines de Paris, France.

Cunningham, C.V.B. 2005. The Kuz-Ram fragmentation model - 20 years on. In R. Holmberg (ed.), *Proc. 3rd EFEE World Conf. on Explosives and Blasting*, Brighton, UK, 13-16 September, pp. 201-210. EFEE.

Hunter, G.C., McDermott, C., Miles, N.J., Singh, A. & Scoble, M.J. 1990. A review of image analysis techniques for measuring blast fragmentation. *Mining Science and Technology* 11(1): 19-36.

Kemeny, J., Girdner, K., Bobo, T. & Norton, B. 1999. Improvements for fragmentation measurement by digital imaging: Accurate estimation of fines. *Proc. 6th Int. Symp. Rock Fragmentation by Blasting – Fragblast 6*, Johannesburg, South Africa, 8-12 August, pp. 103-110. Johannesburg: South African Institute of Mining and Metallurgy.

Latham, J.P., Maerz, N., Kemeny, J., Noy, M., Schleifer, J. & Tose, S. 2003. A blind comparison between results of four image analysis systems using a photo-library of piles of sieved fragments. *FRAGBLAST – Int. J. for Blasting and Fragmentation* 7(2): 105-132.

Maerz, N.H. 1996. Reconstructing 3-d block size distribution from 2-D measurements. In J. Franklin & T. Katsabanis (eds.), *Proc. FragBlast 5 Workshop on Measurement of Blast Fragmentation*, Montreal, Canada, 23-24 August, pp. 39-43. Rotterdam: Balkema.

Ouchterlony, F., Niklasson, B. & Abrahamsson, S. 1990. Fragmentation monitoring of production blasts at MRICA. *Proc. 3rd Int. Symp. on Rock Fragmentation by Blasting*, Brisbane, Australia, 26-31 August, pp.283-289. Parkville, VIC: The Australasian Institute of Mining and Metallurgy.

Outal, S. 2006. Quantification par analyse d'images de la granulométrie des roches fragmentées: amélioration de l'extraction morphologique des surfaces, amélioration de la reconstruction stéréologique. PhD thesis, École des Mines de Paris, France.

Outal, S., Jeulin, D. & Schleifer, J. 2008. A new method for estimating the 3D size-distribution-curve of fragmented rocks out of 2D images. *Image Analysis and Stereology* 27: 95-105.

Peleg, M. 1996. Determination of the parameters of the Rosin-Rammler and beta distributions from their mode and variance using equation-solving software. *Powder Technology*. 87(2): 181-184.

Pirard, E., Vergara, N. & Chapeau, V. 2004. Direct estimation of sieve size distributions from 2-D image analysis of sand particles. *Proc. Int. Cong. on Particle Technology*, Nuremberg, Germany, 27-29 March.

Santalo, L.A. 1976. *Integral geometry and geometric probability*. London: Addison-Westley.

Schleifer, J. & Tessier, B. 1996. FRAGSCAN: A tool to measure fragmentation of blasted rock. In J. Franklin & T. Katsabanis (eds.), *Proc. FragBlast 5 Workshop on Measurement of Blast Fragmentation*, Montreal, Canada, 23-24 August, pp. 73-78. Rotterdam: Balkema.